Macromolecules

Volume 23, Number 26 December 24, 1990

Block Copolymer Adsorption in a Selective Solvent: A Kinetic Study

A. Johner and J. F. Joanny*

Institut Charles Sadron, CRM-EAHP, 6 rue Boussingault, 67083 Strasbourg Cedex, France

Received February 12, 1990

ABSTRACT: We study the adsorption kinetics of diblock copolymers onto a wall in a highly selective solvent good for the nonadsorbing block B and poor for the adsorbing block A. We consider only the adsorption from a micellar phase. The potential barrier for direct adsorption of chains belonging to micelles is so high that only free chains adsorb on the wall. The adsorption of free chains creates a large region in the vicinity of the wall where the free chains are depleted and where the equilibrium between free chains and micelles is broken. The equilibrium is restored by micelle relaxation through the expulsion of chains one by one. Taking the micelle relaxation into account, we write a diffusion–relaxation equation for the adsorption kinetics and distinguish four different time regimes. In the very early stages the adsorption is dominated by the diffusion of free chains toward the wall; at larger times the limiting step is the expulsion of chains by the micelles; the surface coverage increases then linearly with time and the copolymer builds up a grafted B brush on the wall. When the brush is dense enough, the potential barrier for adsorption of new chains is high and the passage through the barrier becomes the limiting step; the surface coverage increases then very slowly (logarithmically) with time. Finally the coverage relaxes to its equilibrium value but over times that are so long that it is not clear whether the equilibrium can be reached experimentally.

I. Introduction

Adsorption of asymmetric AB block copolymers allows the formation of layers of suitable density and large thickness on solid surfaces and is thus well adapted to achieve colloid stabilization, which is of current interest both for scientists and engineers.[1,2] An adapted insoluble anchor permits surface coating with a B brush even though the B homopolymer would not adsorb from the solvent onto the bare surface without any chemical grafting.[3]

AB diblock copolymers exhibit very specific behaviors, compared to homopolymers, whenever one chooses conditions enhancing the difference between the A and B blocks. This is best illustrated in a highly selective solvent, good for B and poor for A. For a single chain, in an infinitely dilute solution, the A block collapses and forms a small globule whereas the B block is swollen and dangling in the solvent.[4]

Above the critical micellar concentration, Φ_{cmc}, chain association into micelles comes into play: the collapsed A chains form a spherical liquid core, lowering the surface energy between A and the solvent, whereas the partially stretched B chains contribute to a semidilute corona, costing some interaction energy.[4] Compared to short-chain surfactant micelles,[5-7] the cmc for long-chain copolymers is extremely small, typically smaller than 1 μmol/L, the aggregation number is large, and the size distribution of the micelles remarkably peaked around its average. If the core block is not too large ($N_A \ll N_B$), both the critical micellar concentration and the size distribution depend only on the molecular weight of the insoluble block.[4,37] Due to the extremely small values of the cmc, real experiments are always made above the cmc and micelles (or other microphases at higher concentrations) are always present in the solution in practice. Above the cmc, micelles are in equilibrium with the free chains, the free-chain concentration is pinned at the cmc value, and any increase in concentration is due to the formation of new micelles.

The existence of the mesophases plays an important role in the structure of adsorbed layers at thermodynamic equilibrium.[8] During adsorption from the solvent onto a solid wall, the insoluble A blocks form a molten film on the wall, whereas the swollen B sequences build up a hairy brush (Figure 1) grafted on this molten layer. Due to the presence of micelles, the characteristics of the interfacial copolymer layer are almost independent of the total copolymer concentration and essentially depend on the copolymer structure. In an actual experiment the adsorbed brush creates a large potential barrier (much larger than kT) for adsorption of new chains and the equilibrium between the solution and the adsorbed layer is reached after extremely long times. Thus the detailed adsorption kinetics is of special interest.

Adsorption from micellar solutions of short-chain surfactants has been studied for a long time. It is in particular usually assumed that micelles do not directly adsorb on the surface;[9] they, however, may play an indirect role,

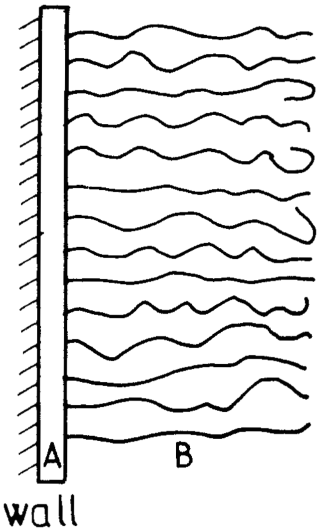

Figure 1. Sketch of the adsorbed block copolymer layer. The A blocks form a molten film, whereas the swollen B blocks build up a brush.

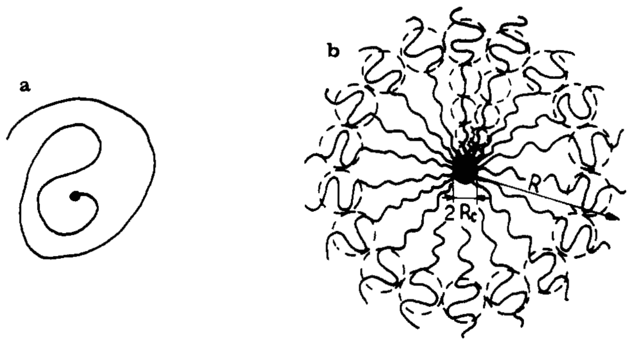

Figure 2. Copolymer micelle (b) and single copolymer chain (a) in a selective solvent. In the free chain the A block is collapsed, whereas the B block is swollen. In the micelle the A blocks form a molten core, whereas the B blocks are partially stretched in the semidilute corona.

releasing free surfactant chains, which may themselves adsorb. Similarly, we investigate here the role of the micelles on diblock copolymer adsorption from a selective solvent. Available experiments on diblock copolymer adsorption kinetics are not numerous. Force measurements between mica plates coated with adsorbed copolymers allow the study of the structure of the layer formed after a chosen incubation time.[3,10–12] Dynamic estimates of the coverage using optical techniques[13] show that above the cmc micelles increase the adsorption rate; the adsorption kinetics clearly displays several regimes and strongly differs from usual homopolymer adsorption kinetics. In particular, equilibrium is approached through an unusually slow process.

In this paper, we propose a kinetic model for diblock copolymer adsorption from a highly selective solvent above the cmc onto a flat solid surface. We consider only asymmetric copolymers that form starlike micelles, where the molecular weight of the insoluble block N_A is smaller than that of the soluble block N_B; the opposite limit where the curvature plays no role in the corona is not considered.

In section II we summarize the micellar solution properties. In particular, we give the micellar size distribution and discuss the relaxation kinetics toward equilibrium of a perturbed size distribution. This follows the work of Aniansson[14–17] for short-chain surfactants recently extended to copolymers by Halperin.[18,19] In section III we examine the interaction between one micelle and the surface in order to investigate direct micellar adsorption. In section IV we introduce the diffusion–relaxation equation for the free-chain concentration in a micellar solution and discuss the boundary conditions at the wall. Section V is devoted to the detailed description of the adsorption kinetics and distinguishes four adsorption regimes: a diffusive regime (V1), a micelle relaxation limited regime (V2), a brush-limited regime (V3), and the final relaxation toward equilibrium (V4). Section VI summarizes the main results and gives some possible issues.

II. Micellar Solution

Although other limits may be of interest, we consider here only the case of segregating A and B blocks in a highly selective solvent, good for B and poor for A. Thus A blocks have a tendency to form molten regions[20] impenetrable for the B block and the solvent, whereas B blocks are swollen.

For an isolated copolymer the A block is collapsed of radius $R_A \simeq N_A^{1/3} a$ and the surface energy between A and the solvent is the dominant contribution to the chemical potential of free chains

$$\mu_1 = kT \log \Phi_1 + 4\pi\gamma_{AS} a^2 N_A^{2/3} \qquad \text{(II-1)}$$

where Φ_1 is the copolymer concentration expressed as a number of chains per unit volume and γ_{AS} the surface tension between A and the solvent. In eq 1 we take the melt as a reference state for the A block and the swollen state for the B block. In all the following R_B denotes the swollen radius of the B chain: $R_B \simeq N_A^{3/5} a$.

Above the cmc aggregation occurs. We first briefly review the micelle size distribution[4,21,22] along the line of ref 4 and then discuss micelle relaxation following the theory of Aniansson.[15–17]

(1) Critical Micellar Concentration in the Bimodal Approximation. We consider one micelle in a free-chain solution that imposes the chemical potential, μ_{ext}, and the osmotic pressure, Π_{ext} (Figure 2). μ_{ext} and Π_{ext} being fixed, the micelle is described by the grand canonical free energy

$$\Omega(p) = F_M(p) - \mu_{ext} p + \frac{4}{3}\pi\{(R_C + L)^3 - R_C^3\}\Pi_{ext} \qquad \text{(II-2)}$$

where $F_M(p)$ is the free energy of a micelle of p chains, R_C the radius of the core, and L the size of the external corona.

The dominant contributions to the free energy are the surface energy between the A core and the solvent and the stretching energy of the B chains in the corona.

$$F_M(p) = 4\pi\gamma_{AS} R_C^2 + F_B \qquad \text{(II-3)}$$

In a good solvent F_B is estimated by using the Daoud and Cotton blob model[23]

$$F_B = kTp^{3/2} \log (N_B^{3/5}/N_A^{1/3} p^{2/15}) \qquad \text{(II-4)}$$

For high enough concentrations (or chemical potential, μ_{ext}) $\Omega(p)$ has a minimum corresponding to a stable micelle. The critical micellar concentration is thus given by

$$d\Omega/dp = 0$$

$$\Omega = 0 \qquad \text{(II-5)}$$

This leads to the optimum aggregation number, cmc and chemical potential:

$$p = N_A^{4/5}\left[\frac{\gamma_{AS}a^2}{kT\log(N_B^{3/5}p^{-2/15}N_A^{-1/3})}\right]^{6/5} \quad \text{(II-6)}$$

$$\Phi_{cmc} = \exp(-4\pi(\gamma_{AS}a^2/kT)N_A^{2/3} + \mu_{cmc}/kT) \quad \text{(II-7)}$$

$$\mu_{cmc} = kTN_A^{2/5}\left(\frac{\gamma_{AS}a^2}{kT}\right)^{3/5}[\log N_B^{3/5}p^{-2/15}N_A^{-1/3}]^{2/5} \quad \text{(II-8)}$$

In most of the following we will for simplicity ignore the logarithms and replace them by constants. The quantities of interest turn out to depend only on N_A apart from the slow logarithmic variations. This is due to the asymmetry of the polymer ($N_B \gg N_A$). The core radius, R_C, is much smaller than the corona thickness, L, and the B blocks in the corona are stretched only in the vicinity of the core. Notice also that the aggregation number is large and the cmc exponentially small.

(2) Micelle Size Distribution. The discussion of the stability of a unique micelle in the reservoir of free chains gives the cmc and the average micelle size; we have, however, ignored the micelles' polydispersity that we now briefly discuss. Let Φ_n be the number of micelles with aggregation number n per unit volume; the grand canonical free energy density per unit volume of the solution reads

$$G = F_{mix} + \sum_n F_M(n)\,\Phi_n - \sum_n n\Phi_n\mu_{ext} + \Pi_{ext} \quad \text{(II-9)}$$

where the free energy of mixing is

$$F_{mix} = kT\sum_n \Phi_n \log(\Phi_n a^3) \quad \text{(II-10)}$$

Interactions between micelles are ignored in eq II-9, which is a good approximation at low concentrations. The free energy must be minimized with respect to Φ_n to obtain the size distribution:

$$\Phi_n a^3 = \exp\left[-\frac{F_M(n) - n\mu_{ext}}{kT} - 1\right] \quad \text{(II-11)}$$

The chemical potential is then obtained by writing the conservation of the total copolymer concentration:

$$\sum_n n\Phi_n = \Phi \quad \text{(II-12)}$$

Minimizing the total free energy GV with respect to the volume V gives the osmotic pressure:

$$\Pi_{ext} = kT\sum_n \Phi_n \quad \text{(II-13)}$$

In general, the size distribution Φ_n is roughly bimodal, as sketched in Figure 3; it contains free chains ($n = 1$) and micelles with an aggregation number n close to the average value $n = p$. The argument of the exponential in the size distribution (eq II-11) is equal to $\Omega(n)$, and thus the argument and its derivative with respect to n become zero for $n = p$ when $\mu_{ext} = \mu_{cmc}$. In the micellar phase, the size distribution is expected to be peaked around its maximum value, and we approximate it by a Gaussian function. Expanding the argument of the exponential to second order around $n = p$ and $\mu_{ext} = \mu_{cmc}$, we get

$$\Phi_n a^3 = \exp\left[-\frac{(n-p)^2}{2\delta p^2} - \frac{(\mu_{cmc} - \mu_{ext})}{kT}p\right] \quad \text{(II-14)}$$

where δp is obtained from the second derivative of $\Omega(n)$ at $n = p$:

$$\delta p = p^{1/4} \simeq N_A^{1/5} \quad \text{(II-15)}$$

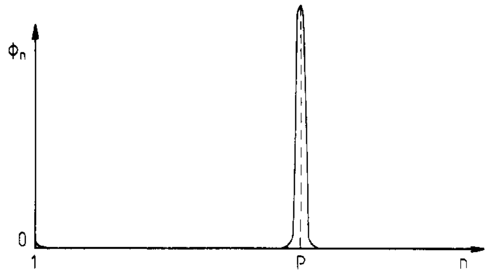

Figure 3. Micelle size distribution, Φ_n. The distribution is almost bimodal, containing free chains and micelles with an aggregation number close to the mean value p.

The concentration of free chains is given by

$$\Phi_1 a^3 = \exp[-(4\pi\gamma_{AS}a^2N_A^{2/3} - \mu_{cmc})/kT] \quad \text{(II-16)}$$

and can be neglected in the total copolymer concentration (eq II-12) in the micellar phase. We then get, summing over the peak of the distribution

$$\Phi_p = \frac{\Phi}{(2\pi)^{1/2}p\,\delta p} \quad \text{(II-17)}$$

Comparison with eq II-14 leads to

$$\frac{\mu_{ext} - \mu_{cmc}}{T} = \frac{1}{p}\log\left(\frac{\Phi a^3}{(2\pi)^{1/2}p\,\delta p}\right) \quad \text{(II-18)}$$

This last equation shows that μ_{ext} is close to μ_{cmc} at the cmc and almost independent of the total concentration, Φ, above the cmc. Inserting μ_{ext} in the expression of the free-chain concentration (eq II-16), we obtain

$$\Phi_1 a^3 = \left[\frac{\Phi a^3}{(2\pi)^{1/2}p\,\delta p}\right]^{1/p}\exp\left(-\frac{4\pi\gamma_{AS}a^2N_A^{2/3} - \mu_{cmc}}{kT}\right) \quad \text{(II-19)}$$

The large value of the aggregation number p keeps the preexponential factor close to unity. As expected, above the cmc, Φ_1 is roughly independent of the total copolymer concentration Φ and close to Φ_{cmc}. In the following we will replace Φ_1 by Φ_{cmc} and μ_{ext} by μ_{cmc} for concentrations above the cmc.

In between $n = 1$ and the central peak $n = p$, the concentration falls dramatically. The minimum value of Φ_n may be estimated as

$$\Phi_n = \left[\frac{\Phi a^3}{(2\pi)^{1/2}p\,\delta p}\right]^{n/p}\exp(-\Omega_{max}/kT); \quad n = n_{min} \quad \text{(II-20)}$$

This extremely low concentration is due to the large value of the maximum of the micelle free energy $\Omega_{max} \simeq 4\pi\gamma_{AS}a^2N_A^{6/5}/kT$, which creates a very high barrier to micelle destruction.

(3) Micelle Relaxation. When the local free-chain concentration falls below the cmc, micelles become unstable; they have to relax. More precisely the whole micelle distribution relaxes. We are here interested in the characteristic times of this relaxation because they are involved in the adsorption kinetics.

In a beautiful series of papers, Aniansson has studied the relaxation of the micelle distribution for micelles of short-chain surfactants.[14-17] We here summarize some of his results: in the last section we will consider more specifically the case of copolymer micelles.

Aniansson distinguishes two relaxation processes: (i) a fast process where relaxation takes place within the central peak of the micelle size distribution (A micelle releases only a few chains, and the total number of micelles remains constant during the fast process.); (ii) a slow process, involving the whole micelle distribution (During the slow process micelles are entirely renewed and the total number of micelles changes. The slow process involves two mechanisms, the emptying chain by chain of the micelle that was originally introduced by Aniansson and a micelle fission process that was considered only later.[24]).

Using chemical kinetics models, Aniansson has computed the relaxation times, T_1 (fast process) and T_2 (slow process), corresponding to his model; these times are defined from the chain creation rate by

$$\frac{\mathrm{d}\Phi_1}{\mathrm{d}t} = -\frac{(\Phi_1 - \Phi_{\mathrm{cmc}})}{T_{1,2}} \qquad \text{(II-21)}$$

The relaxation times depend upon both the average extraction time, τ, of a single chain and the micellar size distribution.

(i) Fast Process. It corresponds to a relaxation mechanism where the micelles remain close to the average composition and only exchange a few chains with the solution. The corresponding relaxation time is given by

$$\frac{1}{T_1} = \frac{\tau^{-1}}{\delta p^2} + \frac{\tau^{-1}}{p}\left(\frac{\Phi_1 - \Phi_{\mathrm{cmc}}}{\Phi_{\mathrm{cmc}}}\right) \qquad \text{(II-22)}$$

where τ is the time for a single chain to leave a micelle, averaged over the peak of the size distribution.

(ii) Slow Process. In his original work Aniansson considers chain by chain emptying of the micelles; the limiting stage involves micelles close to the minimum of the size distribution. The slow-process relaxation time is given by

$$\frac{1}{T_2} = \frac{1}{R\Phi_{\mathrm{cmc}}} \frac{p/\left[\dfrac{\Phi - \Phi_{\mathrm{cmc}}}{\Phi_{\mathrm{cmc}}}\right] + \langle n^2 \rangle}{1 + (\delta p^2/p)\dfrac{\Phi - \Phi_{\mathrm{cmc}}}{\Phi_{\mathrm{cmc}}}} \qquad \text{(II-23)}$$

where τ_n is the extraction time from a micelle of n chains. The rate constant $R = \sum_n \tau_n/\Phi_n$ is dominated by the minimum of the size distribution where Φ_n takes very low values. The relaxation time T_2 contains thus an exponential factor $\exp(\Omega_{\max}/kT)$ involving the maximum of the free energy for a micelle.

In the fission process, introduced by Lessner et al.,[24] the micelle splits into smaller pieces and has to overcome the potential barrier, $\Omega_{\max}$, which introduces again a factor $\exp(\Omega_{\max}/kT)$. The slow process is dramatically slower than the fast process because it involves micelles outside of the central peak of the size distribution.

All these expressions assume a linear relaxation in the chain creation rate (eq II-21). If the departure from equilibrium is large, we must also consider nonlinear relaxation. We do it here only for the fast process, which is relevant for our purpose, and write the relaxation law

$$\mathrm{d}f/\mathrm{d}t = -s(f) \qquad \text{(II-24)}$$

where s is only a function of the reduced concentration, $f = (\Phi_{\mathrm{cmc}} - \Phi_1)/\Phi_{\mathrm{cmc}}$, and of the total concentration, Φ, which remains roughly constant during the fast process. Aniansson gives the first-order expansion of $s(f)$. In the following we use the linear approximation for $s(f)$, which allows for complete calculations. When necessary, we give then the results for the general nonlinear process characterized by $s(f)$, although its precise shape is not known so far to our knowledge (see Appendix III).

(4) Copolymeric Micelle Relaxation. We now focus on starlike copolymer micelles. The extraction time of a single chain has been computed by Halperin,[19] taking into account the potential barrier that prevents one A block from leaving the core of the micelle and the diffusion through the corona, we simply quote his result, but we keep a correction term in the activation energy because in the calculation of T_1 the leading terms cancel:

$$\tau^{-1} = N_{\mathrm{A}}^{-2/25} N_{\mathrm{B}}^{-9/5} \exp\left(-\frac{4\pi N_{\mathrm{A}}^{2/3}\gamma_{\mathrm{AS}}a^2}{kT} + \frac{2\pi}{3}\frac{N_{\mathrm{A}}^{2/3}p^{-1/3}\gamma_{\mathrm{AS}}a^2}{kT}\right)\tau_0 \qquad \text{(II-25)}$$

The exponential factor comes from the potential barrier (it includes the second term in the argument in contrast to ref 19); τ_0 is a microscopic time for a monomer. The relaxation times involve the micelle size distribution; for copolymer micelles this distribution is strongly peaked around its average value. Above the cmc, the free-chain concentration remains close to the unusually small Φ_{cmc}; in actual experiments the concentration of free chains may thus be neglected with respect to the total copolymer concentration, Φ. With these approximations we now calculate the relaxations times, T_1 and T_2.

(a) Relaxation Time, T_1, of the Fast Process. From eq II-22, we obtain

$$\frac{1}{T_1} = \tau^{-1}\frac{\Phi}{\Phi_{\mathrm{cmc}}}p^{-1} \qquad \text{(II-26)}$$

where even for fairly dilute solutions (provided $\Phi \gg \Phi_{\mathrm{cmc}}N_{\mathrm{A}}^{2/5}$) the last term in eq II-23 has been neglected (we consider this limit from now on in contrast with ref 19 where the very vicinity of the cmc is considered). Note that τ^{-1} and Φ_{cmc} both have a decreasing exponential contribution (eqs II-7 and II-25), which should be compared. The leading terms in the exponentials represent both the surface energy of an isolated collapsed A block; they thus cancel. In both arguments the next order term goes as $N_{\mathrm{A}}^{2/5}$ and accounts for the variation of surface energy when a new chain is added to the micelle, but in the chemical potential entering Φ_{cmc} some extra energy is due to the stretching of the B blocks. The exponential arising from Φ_{cmc} thus dominates.

Further, inserting expression II-25 for τ, we obtain

$$T_1 = \frac{N_{\mathrm{A}}^{22/25}N_{\mathrm{B}}^{9/5}}{\Phi a^3}\exp(\alpha N_{\mathrm{A}}^{2/5})\tau_0 \qquad \text{(II-27)}$$

We also note that if we write $\mu_{\mathrm{cmc}} = \beta N_{\mathrm{A}}^{2/5}$, $\alpha < \beta$. For reasonable values of the parameters we expect T_1 to lie in the minute range. In practice, T_1 may become larger if the core is in a glassy state.

(b) Relaxation Time T_2 of the Slow Process. In the expression II-23 for T_2 the limiting factor is the large R due to the extremely small concentration of micelles outside of the central peak of the distribution (eq II-20)

$$T_2 = \tau\frac{\Phi\delta p^2}{\Phi_{\mathrm{min}}p^2} \qquad \text{(II-28)}$$

Taking into account eq II-20, we obtain

$$T_2 \simeq \exp\left(\frac{4\pi\gamma_{\mathrm{AS}}a^2N_{\mathrm{A}}^{6/5}}{T}\right)\tau_0 \qquad \text{(II-29)}$$

For reasonable values of N_{A} the exponential appearing in eq II-29 takes prohibitive values. Thus the slow process should not be observed.

In the characteristic time for the fission process the same exponential appears due to the potential barrier, $\Omega_{\max}$ (see eq II-20): this slow process should not be observed either.

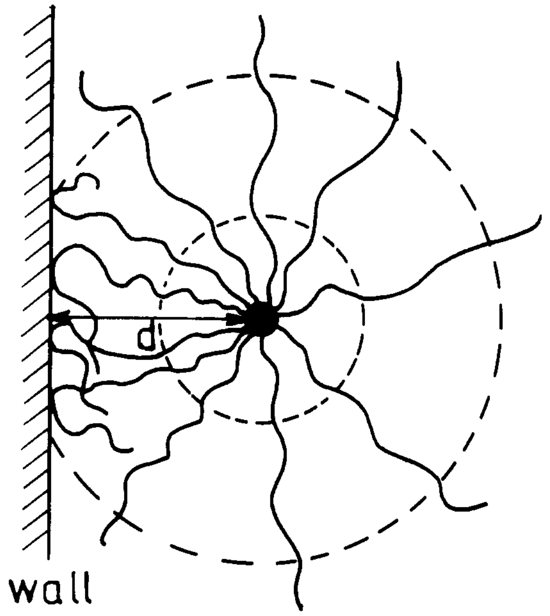

Figure 4. Representation of a starlike micelle, whose core is located at a distance d from the wall.

III. Micelle–Wall Interaction

In this section we consider one micelle close to the wall (Figure 4). In order to bring its core in contact with the wall, the micelle has to overcome a potential barrier due to the B block corona. Here we want to evaluate the height of this barrier. In order to investigate the strength of the interaction as a function of the distance, d, between the core and the wall, we first use a scaling argument for the probability, $P(d)$, to find a micelle at a distance d, following an idea introduced by Witten et al.[25] for the interaction between micelles; we then adapt the Daoud and Cotton[23] blob model to this particular geometry. The two arguments lead to an interaction decreasing logarithmically with distance. This result is also true in a mean-field model as shown in Appendix I.

(1) Scaling Argument. We expect that the interaction between the micelle and the wall decays rapidly for distances larger than the micelle radius, R. The probability, $P(d)$, of finding a micelle at a distance d from the wall then becomes d independent. Closer to the wall we assume a scaling law for $P(d)$. We thus write the probability ratio, $P(d)/P(\infty)$, as

$$P(d)/P(\infty) = 1 \qquad \text{for } d \gg R$$

$$P(d)/P(\infty) \simeq (d/R)^m \qquad \text{for } d \ll R \qquad \text{(III-1)}$$

where m is an exponent to be determined. The probability ratio is equal to the corresponding partition function ratio:

$$P(d)/P(\infty) = Z(d)/Z(\infty) \qquad \text{(III-2)}$$

where $Z(d)$ is the partition function of a micelle at a distance d from the wall. We can rewrite this relation in terms of the free energy $F(d)$ of the micelle

$$\log\,(P(d)/P(\infty)) = -(kT)^{-1}(F(d) - F(\infty)) = -U(d)/kT \qquad \text{(III-3)}$$

where $U(d)$ is the interaction energy between the micelle and the wall. As long as the A core of the micelle is not in contact with the wall we assume that the free-energy variation is mainly due to the changes in the free energy of the B block corona. For the special case where d is of the order of the core radius, R_C, the free-energy variation at the right-hand side of III-3 can be estimated in the Daoud and Cotton[23] blob model. When $d \simeq R_C$, the original grafting density, σ, is roughly doubled in the remaining half-space, taking into account only the stretching energy, F_B, of the B blocks:

$$F(R_C) - F(\infty) = 0.5F_B(2\sigma) - F_B(\sigma) \simeq kTp^{3/2}\log\,(R/R_C) \qquad \text{(III-4)}$$

From eq III-3 the probability ratio is $P(R_C)/P(\infty) \simeq (R_C/R)^{p^{3/2}}$. We thus obtain the exponent $m \simeq p^{3/2}$. The mean interaction between a micelle and the wall is thus

$$U(d) \simeq -kTp^{3/2}\log\,(d/R) \qquad \text{(III-5)}$$

The interaction energy reaches a maximum value when the core of the micelle is in contact with the wall.

$$U_{\max} = U(R_C) = -kTp^{3/2}\log\,(R_C/R) \qquad \text{(III-6)}$$

The radius R of the micelle far away from the wall is given by the Daoud and Cotton model.[23]

$$R = R_B p^{1/5} \simeq N_B^{3/5} N_A^{4/25} a \qquad \text{(III-7)}$$

The core radius is

$$R_C = (pN_A)^{1/3} a = N_A^{3/5} a \qquad \text{(III-8)}$$

The energy barrier for a micelle to bring its core in contact with the wall is thus

$$U_{\max}/kT = N_A^{6/5}\log\,(N_B^{3/5} N_A^{-11/25}) \qquad \text{(III-9)}$$

In the early stages of the adsorption, the flux of micelles toward the wall has a contribution proportional to $\exp(-U_{\max}/kT)$. This is to be compared with the flux of free chains toward the wall, which is also exponentially small because of the small value of the free-chain concentration in the bulk, Φ_{cmc}. However, Φ_{cmc} is proportional to $\exp(-\gamma_{AS} N_A^{2/3} a^2/T)$, and if in a first approximation, we compare the exponential factors entering the two fluxes, at the beginning of the adsorption, the flux of chains carried in micelles toward the wall is much smaller than the flux of free chains. We may thus ignore the direct adsorption of micelles and from now on we will assume that only the free chains adsorb on the wall.

(2) Daoud–Cotton Model. Equation III-5 for the interaction energy has been obtained through a scaling law. We now rederive it by using a slightly modified version of the blob model of Daoud and Cotton. In the original Daoud–Cotton model,[23] the spherical symmetry allows an elegant calculation of the stretching energy in the corona of an isolated micelle considered as a starlike polymer. At a distance r from the center, each B block crosses once the sphere of radius r and occupies an area $\xi^2(r) = 4\pi r^2/p$ where ξ is the local blob size (or correlation length). Here we perform an analogous calculation, assuming that the mean effect of the wall results in a truncation of the largest of these spheres. Assuming that each B block crosses any of these surfaces, p blobs must accommodate on any one. $S(r)$ being the area of the surface of radius r, the correlation length, $\xi(r)$, is given by

$$\xi(r) = (S(r)/p)^{1/2} \qquad \text{(III-10)}$$

When the center of the A core of the micelle is located at a distance d, smaller than R, from the wall, the micelle may be divided into two regions. In the inner region ($r < d$) the surfaces are spheres, whereas in the outer regions they are truncated spheres:

$$S(r) = 4\pi r^2 \qquad \text{for } r < d$$

$$S(r) = 2\pi(1 + d/r)r^2 \qquad \text{for } r > d \tag{III-11}$$

In the semidilute corona the local concentration is related to the correlation length by

$$c(r) \simeq \xi^{-4/3} \tag{III-12}$$

The total number of B monomers in the corona is thus given by

$$N_{\mathrm{B}}p = \int_{R_{\mathrm{C}}}^{R(d)} S(r)\,(S(r)/p)^{-2/3}\,\mathrm{d}r \tag{III-13}$$

This gives the radius $R(d)$ of the micelle at a distance d from the wall. $R(d)$ differs only from $R(\infty)$ through a numerical factor, in particular for $d \ll R(\infty)$:

$$R(d) = 2^{1/5}R(\infty)(1 + O(d/R(\infty))) \tag{III-14}$$

The free energy $F(d)$ of a micelle at a distance d from the wall is obtained by summing the local free-energy density $T/\xi(r)^3$:

$$F(d) = kT\int_{R_{\mathrm{C}}}^{R(d)} p^{3/2}S(r)^{-1/2}\,\mathrm{d}r \tag{III-15}$$

Only the outer region ($r > d$) of the micelle contributes to the free-energy variation and

$$U(d) = F(d) - F(\infty) = kTp^{3/2} \times \left\{\int_d^{R(d)} \frac{\mathrm{d}r}{(2\pi(1 + d/r)r^2)^{1/2}} - \int_d^{R(\infty)} \frac{\mathrm{d}r}{(4\pi r^2)^{1/2}}\right\} \tag{III-16}$$

Finally for $d \ll R(\infty)$ we obtain

$$U(d) = -kTp^{3/2}(2\pi)^{-1/2} \times \left\{\ln\left[\frac{(3 + 2^{3/2})d}{(4)(2^{1/5})R(\infty)}\right] - 2^{-1/2}\ln\left[\frac{d}{2^{1/5}R(\infty)}\right]\right\} \tag{III-17}$$

This result is consistent with the previous scaling form III-5. Although this is still an approximation, the spherical symmetry being certainly broken for a micelle close to the wall, it allows an estimation of the numerical constants.

IV. Adsorption Kinetics

In this section we present the diffusion–relaxation equation for the free-chain concentration (IV1) in the bulk solution and the diffusion–convection equation for the chain concentration in the brush near the wall (IV2). We then replace the adsorbed layer brush by the appropriate boundary conditions for the diffusion problem.

(1) Diffusion–Relaxation Equation in the Solution. From the previous section we know that only free chains adsorb from the solution onto the wall. At the early stages of adsorption, free chains diffuse to the surface with a diffusion coefficient D and adsorb. The resulting diffusive free-chain concentration profile presents a depletion layer of width $(Dt)^{1/2}$ after a time t and goes to the cmc far from the wall.[26-28] Within this hole the free-chain concentration falls below the cmc, the micelles located close to the wall become unstable and relax. Micelles play thus an indirect role in the adsorption process, releasing free chains that may themselves adsorb. Micelle relaxation occurs through Aniansson's fast process, which leaves the micelle concentration constant and introduces only a negligible change for the micelle polydispersity. We may thus assume a constant micelle concentration without any diffusion or interdiffusion process. We then write the diffusion equation for free chains including a source term due to micelle relaxation. This term depends on the difference between the actual local chain concentration and the cmc

$$\frac{\partial f}{\partial t} = D\frac{\partial^2 f}{\partial z^2} - s(f) \tag{IV-1}$$

where $f = (\Phi_{\mathrm{cmc}} - \Phi_1)/\Phi_{\mathrm{cmc}}$ is the reduced free-chain concentration. For low f the micelle relaxation term $s(f)$ is linear in f and is given by

$$s(f) = f/T_1 \tag{IV-2}$$

The local chain flux, J, is

$$J = D\Phi_{\mathrm{cmc}}\frac{\partial f}{\partial z} \tag{IV-3}$$

Far from the wall Φ_1 remains fixed at Φ_{cmc} so that

$$\lim_{z \to \infty} f = 0 \tag{IV-4}$$

In the next subsection we investigate chain diffusion in the brush near the wall in order to determine the appropriate boundary condition of this diffusion problem in the bulk solution.

(2) Diffusion–Convection Equation in the Brush near the Wall. During the early stage of copolymer adsorption the isolated swollen B sequences dangle in the solution forming "buoys" fixed on the adsorbed A "anchor". When the surface coverage, σ, increases, the B blocks, because of the excluded-volume interaction, stretch and form a brush.[29] The crossover to this brush regime occurs when the swollen B blocks come into "contact"; i.e., at the overlap coverage $\sigma_0 a^2 \simeq N_{\mathrm{B}}^{-6/5}$. The resulting brush may in a first approximation be described by a blob model first proposed by Alexander, which will be sufficient for our purpose.[30]

A chain in the brush remains locally isotropic at scales smaller than $\sigma^{-1/2}$, whereas at larger scales it is stretched. One chain in the brush is thus viewed as a stretched chain made of $N_{\mathrm{B}}/(\sigma a^2)^{-5/6}$ isotropic swollen blobs each of size $\sigma^{-1/2}$. The thickness L of the brush is given by

$$L = N_{\mathrm{B}}(\sigma a^2)^{1/3}a \tag{IV-5}$$

The energy per blob is kT, and the stretching energy F of one chain is

$$F = kTN_{\mathrm{B}}(\sigma a^2)^{5/6} \tag{IV-6}$$

A nonadsorbed chain is also stretched when it enters the brush. A free chain coming from the solution has to overcome a barrier of order F to adsorb. To enter the brush, a micelle would have to overcome a repelling potential barrier of height of order pF; we may thus neglect micelles in the brush.

The diffusive motion of a chain in the brush is a reptative motion in a tube of section σ^{-1}.[38] Even at equilibrium the blob size $\sigma^{-1/2}$ remains larger than the radius of the collapsed A block; thus the A block is free in the brush. When n monomers of the B block are inside the brush, the mobility, Λ, of the copolymer is in the reptation model given by

$$\Lambda^{-1} = 6\pi\eta n\sigma^{-1/2}(\sigma a^2)^{5/6} \tag{IV-7}$$

η being the solvent viscosity.

If part of the B block in the brush extends between distances z and L from the wall, $L - z = n\sigma^{-1/2}(\sigma a^2)^{5/6}$, the mobility is

$$\Lambda^{-1}(z) = 6\pi\eta(L - z) \qquad \text{for } z < L \text{ and } (L - z)/L \simeq 1 \tag{IV-8}$$

The Einstein relation gives the diffusion coefficient $D(z)$:

$$D(z) = kT\Lambda(z) \qquad \text{(IV-9)}$$

The insertion of a portion of a B block inside the brush requires an energy of order kT for each new blob; the total free energy cost $F(z)$ is thus

$$F(z) = kT\sigma^{1/2}(L - z) \qquad \text{(IV-10)}$$

In the brush the diffusing chain moves under a driving force $-\partial F/\partial z$ arising from the repulsive brush potential. We thus write, a diffusion-convection equation for the chain concentration in the brush

$$\frac{\partial \Phi_1}{\partial t} = \frac{\partial}{\partial z}\left(D(z)\frac{\delta \Phi_1}{\delta z}\right) + \frac{\partial}{\partial z}\left(\Phi_1 D(z)\frac{\delta U}{\delta z}\right) \qquad \text{(IV-11)}$$

where $U(z) = F(z)/kT$.

The flux of chains inside the brush is given by

$$J = -D(z)\left\{\frac{\partial \Phi}{\partial z} + \Phi_1\frac{\partial U}{\partial z}\right\} \qquad \text{(IV-12)}$$

The conservation of the chains at the wall relates the flux on the wall to the surface coverage σ (expressed as a number of chains per unit area).

$$\frac{\mathrm{d}\sigma}{\mathrm{d}t} = -J|_{\text{wall}} \qquad \text{(IV-13)}$$

We then have to write the adsorption equilibrium at the wall for chains that go through the brush. We assume that the adsorption occurs locally at thermodynamic equilibrium so that the chemical potentials of adsorbed and nonadsorbed chains at the wall are equal.

$$\mu_{\text{ch}}|_{\text{wall}} = \mu_{\text{ads}}|_{\text{wall}} \qquad \text{(IV-14)}$$

We represent the interfacial brush by a repulsive potential barrier for an incoming chain; behind the brush the A film and the wall are replaced by a free-chain solution of concentration Φ_s where Φ_s would be in equilibrium with the interface of coverage σ. Far from equilibrium between the interface and the bulk solution Φ_s may be set equal to zero, neglecting any desorption or saturation effect. As we will see later for copolymer adsorption the repelling brush potential is so large the saturation effects only become relevant very close to thermodynamic equilibrium, which is reached very slowly, so that the domain where Φ_s remains negligible extends to very long times.

For most of the adsorption process, the concentration in the brush may be assumed to be steady. The flux J given by eq IV-12 is then roughly constant throughout the brush so that

$$\frac{\partial \Phi_1}{\partial z} + \Phi_1\frac{\partial U}{\partial z} = -\frac{J}{D(z)} \qquad \text{(IV-15)}$$

After integration eq IV-15 gives

$$J = -\frac{\Phi_0 - \Phi_s}{\displaystyle\int_0^L \frac{\exp(U(z))}{D(z)}\,\mathrm{d}z} = -K(\Phi_0 - \Phi_s) \qquad \text{(IV-16)}$$

where Φ_0 is the concentration of free chains near the brush on the solution side.

Taking eqs IV-8 and IV-10 into account, we obtain the following expression for the transparence K:[31]

$$K = \frac{kT(\sigma a^2)^{1/6}}{6\pi\eta N_B a^2}\exp(-N_B(\sigma a^2)^{5/6}) \qquad \text{(IV-17)}$$

So far this section has dealt only with well-covered surfaces $\sigma > N_B^{-6/5}$ to obtain the above results for the boundary condition at the wall. From the crossover to the low-coverage limit we obtain

$$K = D/R_B \quad \text{for } \sigma < N_B^{-6/5} \qquad \text{(IV-18)}$$

It is not clear whether this expression and the associated Zimm time make any sense for very low coverages for which other microscopic times such as an adsorption time should be considered. However, it will turn out that K is never a relevant parameter in the low-coverage regimes.

Equation IV-16 may now be considered as a boundary condition for the bulk diffusion equation (eq IV-1). This allows the study of the adsorption kinetics of block copolymers.

V. Adsorption from a Micellar Solution

The adsorption of a copolymer solution on a solid wall leads to the formation of an interfacial layer between the wall and the solution.[8,32] The double-layer structure of this interface at thermodynamic equilibrium, sketched on Figure 1, has been extensively studied by Marquès, Joanny, and Leibler;[8] we quote here some of their results. The main parameter governing the structure of the layer is the asymmetry of the copolymer chain, measured by the ratio between the A block radius in the molten state and the B block radius in the swollen state:

$$\beta_s = N_B^{3/5}/N_A^{1/2} \qquad \text{(V-1)}$$

A detailed analysis of the different contributions to the free energy of the layer shows the following:

(1) For large B blocks ($\beta_s \gg N_A^{7/50} \simeq 1$) the van der Waals energy of the A film and the stretching energy of the B brush dominate.

(2) In a small domain ($\beta_s \simeq 1$) the stretching energy of the brush dominates. At thermal equilibrium with a micellar solution this gives the coverage σ_{eq}.

(3) For large B blocks ($\beta_s \gg 1$), which mostly is the situation that we consider

$$\sigma_{\text{eq}}a^2 = \left(\frac{AN_A}{kT}\right)^{6/23}\frac{1}{N_A}\beta_s^{-10/23} \simeq N_A^{-12/23}N_B^{-6/23} \qquad \text{(V-2)}$$

A being the Hamacker constant, measuring the strength of the van der Waals interaction. In the last expression we have assumed $(A/kT)^{6/23} \simeq 1$.

(4) For $\beta_s \simeq 1$, a case which may be encountered when $N_A \simeq N_B$

$$\sigma_{\text{eq}}a^2 = N_A^{-12/25}\beta_s^{-2}(\gamma_{AS}a^2/kT)^{18/25} \simeq N_A^{12/25}N_B^{-6/5} \qquad \text{(V-3)}$$

The surface tension, $\gamma_{AS}a^2/kT$, is of order 1.

We now discuss in detail the successive kinetic regimes expected during an adsorption experiment from a micellar copolymer solution onto a wall that leads to this equilibrium structure. At the early stages of the adsorption, the coverage rate is limited by the diffusion of free chains from the solution toward the surface; this we call the diffusive regime (V1). After a time on the order of Aniansson's time, T_1, the micelles in the depletion layer created by the diffusion begin to release free chains, this relaxation process characterized by the time T_1 becomes rate limiting; this we call the micelle-limited regime (V2). When a sufficiently dense brush is formed, the diffusion through the repelling brush potential, characterized by K, becomes the limiting step; this we call the brush-limited regime (V3). For coverages σ approaching the equilibrium coverage, σ_{eq}, saturation effects can no longer be ignored; this we call the saturation regime (V4). However, as we will see, the dense brush close to equilibrium is so much rate limiting that saturation becomes relevant only extremely close to equilibrium.

With the exception of the saturation regime the concentration at the wall behind the brush Φ_s can be neglected in the boundary condition IV-16. The adsorption kinetics is then governed by the following equations: the diffusion–relaxation equation (eq IV-1), the relation between the flux in the solution and the reduced concentration, $f(z)$ (eq IV-3), the boundary conditions at the wall and far away from the wall

$$J(0) = -K\Phi_{\text{cmc}}(1 - f(0)) \text{ and } f(\infty) = 0 \qquad \text{(V-4)}$$

and the chain conservation equation at the wall (eq IV-13).

These equations are solved in detail in Appendix II; we only present here simple arguments giving some physical insight.

(1) Diffusive Regime. At the early stages of the adsorption ($t < T_1$) micelle relaxation is not relevant. The interfacial layer is not formed, and there is no potential barrier to overcome. The adsorption kinetics is thus governed by the diffusion of the free chains toward the surface. In this regime the free-chain concentration at the wall falls to zero and the simpler boundary condition $f(0) = 1$ is used in place of eq V-4.

The problem may be solved by Laplace transformation. Denoting the Laplace transform of a function $h(t)$ of time by $\mathbf{h}(s)$, the diffusion equation becomes

$$s\mathbf{f}(s) = D\mathbf{f}''(s) \qquad \text{(V-5)}$$

so that

$$\mathbf{f}(s) = B(s) \exp(-(s/D)^{1/2}z) \qquad \text{(V-6)}$$

The simplified boundary condition $f(0) = 1$ gives $\mathbf{f}(0) = 1/s$ so that

$$\mathbf{f}(s) = s^{-1} \exp(-(s/D)^{1/2}z) \qquad \text{(V-7)}$$

which in turns leads to the coverage through (eqs IV-3 and IV-13)

$$\sigma(s) = \Phi_{\text{cmc}}D^{1/2}s^{-3/2} \qquad \text{(V-8)}$$

Coming back to the time variable

$$\sigma(t) = 2\Phi_{\text{cmc}}(Dt/\pi)^{1/2} \qquad \text{(V-9)}$$

we recover a square root increase, which is classical for diffusion-controlled adsorption. Due to the extremely small value of the cmc, the coverage remains exponentially low in this regime, which ends at times of order T_1, well in the experimental range.

A more detailed calculation using the original boundary condition V-4 takes into account a molecular potential barrier preventing adsorption and leads to the following expression for the Laplace transform $\sigma(s)$ of the coverage:

$$\sigma(s) = D^{1/2}\Phi_{\text{cmc}}s^{-3/2}(1 + D^{1/2}s^{1/2}K^{-1}) \qquad \text{(V-10)}$$

In addition to the diffusive regime, this expression gives an initial regime, the molecular regime, where $\sigma(s) = K\Phi_{\text{cmc}}s^{-2}$. In this molecular regime the adsorption rate is constant due to the adsorption at the initial chain concentration, Φ_{cmc}, near the wall through the molecular barrier. The crossover between molecular and diffusive regimes is found at $\tau_{\text{micro}} = D/K^2$. $K(\sigma)$ may here be replaced by $K(0)$, which is at least of order D/R_B (eq IV-18), and the molecular crossover time is R_B^2/D. This time describes for example the diffusive rotation bringing the A block to the wall. In practice the chains are not brought to the wall instantaneously at the bulk concentration and also molecular times cannot be investigated experimentally in adsorption kinetics; hence, we start the description with the diffusive regime.

(2) Micelle-Limited Regime. When micelle relaxation becomes relevant, we must incorporate the micelle relaxation term in the diffusion equation for the free chains in eq IV-1. In the vicinity of the solid surface the chain concentration profile is quasisteady at times larger than T_1. We thus neglect the time derivative at the left-hand side of eq IV-1 (the nonsteady profile that is calculated for this regime and the diffusive regime in Appendix II shows how the profile becomes steady near the wall). The diffusion–relaxation equation then reads

$$\mathrm{d}^2f/\mathrm{d}z^2 = f/DT_1 \qquad \text{(V-11)}$$

The concentration profile is then given by

$$f(z) = f(0) \exp(-z/(DT_1)^{1/2}) \qquad \text{(V-12)}$$

$f(0)$ is determined by the boundary condition (V-4) at the wall:

$$f(0) = K/(K + D/(DT_1)^{1/2}) \qquad \text{(V-13)}$$

From $f(z)$ we obtain an equation for the coverage using eqs IV-3 and V-4:

$$\frac{\mathrm{d}\sigma}{\mathrm{d}t} = \frac{\Phi_{\text{cmc}}DK}{(DT_1)^{1/2}(D/(DT_1)^{1/2} + K)} \qquad \text{(V-14)}$$

At small coverages, the characteristic time to cross the potential barrier D/K^2 is small compared to the micelle relaxation time, T_1, the micelle relaxation is the limiting step of the adsorption process, and the transparence, $K(\sigma)$, is large compared to $D/(DT_1)^{1/2}$. This holds for

$$K(\sigma) \gg D/(DT_1)^{1/2} \qquad \text{(V-15)}$$

The surface coverage, σ^*, where the potential barrier characterized by $K(\sigma)$ becomes relevant is obtained from eq IV-17

$$\sigma^*a^2 = N_B^{-6/5}[\ln(T_1/\tau_0)]^{6/5} \qquad \text{(V-16)}$$

where τ_0 is a microscopic time. T_1/τ_0 is exponentially large, and σ^* is always significantly larger than the overlap coverage $\sigma_0 \simeq N_B^{-6/5}a^{-2}$. The brush is already well formed when the potential barrier becomes relevant.

The molecular weight dependence of σ^* is obtained by inserting expression II-27 for T_1

$$\sigma^*a^2 = N_B^{-6/5}N_A^{12/25} \qquad \text{(V-17)}$$

where we have replaced the logarithmic factors by constants in a first approximation. We also check that σ^* is smaller than the equilibrium coverage, σ_{eq}. For an asymmetric block copolymer with $N_B \gg N_A^{16/15}$ the equilibrium coverage is given by eq V-2 so that

$$\sigma^*/\sigma_{\text{eq}} = (N_A^{16/15}/N_B)^{108/115} \ll 1 \qquad \text{(V-18)}$$

The brush potential becomes thus relevant before the coverage reaches the equilibrium value, σ_{eq}.

For less asymmetric block copolymers the equilibrium coverage is given by eq V-3 and the ratio $\sigma^*/\sigma_{\text{eq}}$ is of order 1. In this regime the brush potential may only become relevant for coverages of order σ_{eq}; we however check in Appendix IV that σ^* remains smaller than σ_{eq}.

In the micelle-limited regime the coverage rate (eq V-14) is constant and the coverage σ increases linearly with time.

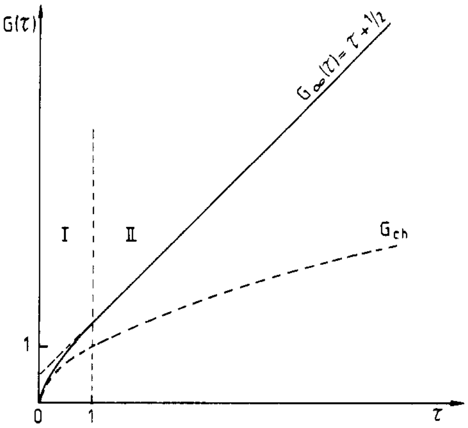

Figure 5. Short-time kinetics. We plot the reduced coverage $G = \sigma/\Phi_{\rm cmc}(DT_1)^{1/2}$ as a function of the reduced time, $\tau = t/T_1$, in the diffusive and micelle-limited regimes as obtained from the explicit calculation in Appendix II. The dashed line corresponds to adsorption without micelle relaxation (- - -, $G_{\rm ch}$).

$$\sigma = \Phi_{\rm cmc}(DT_1)^{1/2}(t/T_1 + c) \qquad \text{(V-19)}$$

The integration constant c of order unity can be neglected at times much larger than T_1 (the detailed calculation in Appendix II gives $c = {}^1/_2$). This linear increase is expected to be valid for times smaller than T_3:

$$T_3 = \frac{N_{\rm B}^{-6/5}a(DT_1)^{1/2}[\ln (T_1/\tau_0)]^{6/5}}{\Phi_{\rm cmc}a^3D} \qquad \text{(V-20)}$$

The molecular weight dependence of T_3 is estimated from that of T_1 and $\Phi_{\rm cmc}$ (eqs II-7 and II-27):

$$T_3 = \frac{N_{\rm A}^{11/25}\exp(\gamma_{\rm AS}(4\pi/3)N_{\rm A}^{2/3} - (\beta - \alpha/2)N_{\rm A}^{2/5})}{(\Phi a^3)^{1/2}} \qquad \text{(V-21)}$$

For consistency we also have to check that the relaxing micelles with a size belonging to the peak of the distribution each release less chains than the average fluctuation, δp, of the distribution. This condition is most restrictive for micelles near the wall for which it can be written as

$$\Phi\, \delta p > \Phi_{\rm cmc}T_3/T_1 \qquad \text{(V-22)}$$

Inserting expressions II-7 for $\Phi_{\rm cmc}$ and II-27 for T_1, we obtain

$$\Phi a^3 > N_{\rm B}^{-18/5}N_{\rm A}^{-6/5}\exp(-\alpha N_{\rm A}^{2/5}) \qquad \text{(V-23)}$$

This condition is not very restrictive and is satisfied at any concentration much larger than the cmc (the only ones of practical interest).

We thus expect a linear increase of the coverage between times T_1 and T_3. In this regime, micelle relaxation is the rate-limiting process. A comparison between eqs V-9 and V-19 shows how micelle relaxation accelerates considerably the adsorption with respect to what it would be for a solution containing only free chains (see also the calculation in Appendix II and the associated Figure 5). We have supposed here that the micelle relaxation is linear. The influence of a nonlinear micelle relaxation on the adsorption is briefly discussed in Appendix III.

(3) Brush-Limited Regime. When the potential barrier due to the brush dominates the kinetics, K may be neglected with respect to $D/(DT_1)^{1/2}$ in eqs V-13 and V-14. The coverage rate given by eq V-14 is

$${\rm d}\sigma/{\rm d}t = K(\sigma)\,\Phi_{\rm cmc} \qquad \text{(V-24)}$$

This is independent of the micelle relaxation time T_1, and the free-chain concentration is very close to the cmc even in the vicinity of the wall. The coverage rate strongly depends on the coverage σ through $K(\sigma)$ that varies essentially exponentially. When eq IV-15 is used for $K(\sigma)$, eq V-24 may be integrated:

$$\sigma a^2 = N_{\rm B}^{-6/5}\{\ln (t/T_4)\}^{6/5} \qquad \text{(V-25)}$$

The characteristic time T_4 in the brush regime is

$$T_4 = \tau_0/(\Phi_{\rm cmc}a^3) \qquad \text{(V-26)}$$

where $\tau_0 = 6\pi\eta a^3/kT$ is a microscopic time.

Note that $\ln (T_3/T_4) = (1/2) \ln (T_1/\tau_0)$ and that eq V-25 crosses over smoothly to the micelle regime coverage at $t = T_3$. In this regime where the kinetics is dominated by the diffusion through the potential barrier, the coverage increases roughly as $\ln t$ and the kinetics is unusually slow. This regime is expected to last until saturation effects come into play, when the extrapolated coverage (eq V-25) becomes close to the equilibrium coverage, $\sigma_{\rm eq}$. We thus define the crossover time T_5 where the extrapolated coverage reaches its equilibrium value.

$$\ln (T_5/T_4) = N_{\rm B}(\sigma_{\rm eq}a^2)^{5/6} \qquad \text{(V-27)}$$

For asymmetric copolymers ($N_{\rm B} > N_{\rm A}^{16/15}$) the equilibrium coverage is given by eq V-2 so that

$$T_5 \simeq \tau_0 \exp[(4\pi/3)\gamma_{\rm AS}N_{\rm A}^{2/3} + N_{\rm B}^{18/23}N_{\rm A}^{-10/23} - \beta N_{\rm A}^{2/5}] \qquad \text{(V-28)}$$

For symmetric copolymers the equilibrium coverage is given by eq V-3 at the crossover, and the two last terms on the right-hand side of eq V-28 cancel leading to

$$T_5 \simeq \tau_0 \exp[(4\pi/3)\gamma_{\rm AS}N_{\rm A}^{2/3}] \qquad \text{(V-29)}$$

A direct comparison between the leading exponential contributions to T_5 (eq V-28 or V-29) and T_3 (eq V-21) shows that $T_5 > T_3$, as expected from the discussion of σ^* (eq V-18). We thus expect a brush-limited regime for times $T_3 < t < T_5$. In many experimental situations, we may also expect that the equilibrium is never reached, the experimental time scale being smaller than T_5.

(4) Saturation. At the end of the brush regime, final relaxation toward equilibrium takes place. In the solution close to the brush the chain concentration is close to $\Phi_{\rm cmc}$, but due to the brush barrier, the coverage is not yet the equilibrium coverage. The flux $J_{\rm s}$ to the wall in the saturation regime is obtained from eq IV-16, assuming that $K(\sigma)$ is approximately equal to its equilibrium value $K_{\rm eq}$:

$$J_{\rm s} = -K_{\rm eq}(\Phi_{\rm cmc} - \Phi_{\rm s}) \qquad \text{(V-30)}$$

The chemical potential, $\mu_{\rm ads}(\sigma)$, for the adsorbed chains at coverage σ is

$$\mu_{\rm ads}(\sigma) = \mu_{\rm cmc} + \left.\frac{\partial\mu_{\rm ads}}{\partial\sigma}\right|_{\rm eq}\delta\sigma \qquad \text{(V-31)}$$

where $\delta\sigma = \sigma - \sigma_{\rm eq}$.

On the other hand, the chemical potential for the free chains at concentration $\Phi_{\rm s}$ is

$$\mu_{\rm ch} = \mu_{\rm cmc} + kT \log (\Phi_{\rm s}/\Phi_{\rm cmc}) = \mu_{\rm cmc} + kT\, \delta\Phi_{\rm s}/\Phi_{\rm cmc} \qquad \text{(V-32)}$$

where $\delta\Phi_{\rm s} = \Phi_{\rm s} - \Phi_{\rm cmc}$.

The adsorbed layer of coverage σ would be at equilibrium with a free-chain solution of concentration $\Phi_{\rm s}$. The relationship between $\delta\Phi_{\rm s}$ and $\delta\sigma$ is obtained by equating

μ_{ads} and μ_{ch}

$$\delta\Phi_s = \frac{\Phi_{cmc}}{kT}\frac{\partial\mu_{ads}}{\partial\sigma}\bigg|_{eq}\delta\sigma \qquad \text{(V-33)}$$

and therefrom the flux J_s to the wall (eq V-30) is

$$J_s = K_{eq}\frac{\Phi_{cmc}}{kT}\frac{\partial\mu_{ads}}{\partial\sigma}\bigg|_{eq}\delta\sigma \qquad \text{(V-34)}$$

The crossover between the brush regime and the saturation regime occurs with a continuous adsorption rate. The crossover coverage is expected to lie close to equilibrium coverage. The flux to the wall at the crossover on the brush regime side is approximately

$$J = -K_{eq}\Phi_{cmc} \qquad \text{(V-35)}$$

Equating the two fluxes $J_s(\sigma^*)$ and $J(\sigma^*)$ gives the relative difference between crossover coverage and equilibrium coverage $\delta\sigma^* = \sigma^* - \sigma_{eq}$:

$$\frac{\delta\sigma^*}{\sigma_{eq}} = \frac{-1}{\sigma_{eq}}\left(\frac{1}{kT}\frac{\partial\mu_{ads}}{\partial\sigma}\bigg|_{eq}\right)^{-1} \qquad \text{(V-36)}$$

The chemical potential in the adsorbed layer may be estimated from the free energy, $F(\sigma)$, of the layer

$$\partial\mu_{ads}/\partial\sigma = \delta F/\delta\sigma = kTN_B\,(\sigma a^2)^{-1/6}a^2 \qquad \text{(V-37)}$$

leading to

$$\delta\sigma^*/\sigma_{eq} = -N_B^{-1}(\sigma_{eq}a^2)^{-5/6} \qquad \text{(V-38)}$$

For symmetric copolymers

$$\delta\sigma^*/\sigma_{eq} = N_A^{-2/5} \ll 1 \qquad \text{(V-39)}$$

For asymmetric copolymers ($N_B \gg N_A^{16/15}$)

$$\delta\sigma^*/\sigma_{eq} = N_A^{-2/5}(N_A^{16/15}/N_B)^{18/23} \ll 1 \qquad \text{(V-40)}$$

Saturation only becomes relevant very close to the equilibrium coverage, σ_{eq}, as expected.

The characteristic relaxation time for this saturation regime is obtained by equating the flux toward the surface with the coverage rate

$$\mathrm{d}\delta(\sigma a^2)/\mathrm{d}t = \delta(\sigma a^2)/T_6 \qquad \text{(V-41)}$$

where the relaxation time T_6 is given by

$$T_6 = \{K_{eq}N_B(\sigma_{eq}a^2)^{-1/6}\Phi_{cmc}a^2\}^{-1} \qquad \text{(V-42)}$$

This time has the same exponential molecular weight dependence as T_5. At even larger times, outside the experimental range, micelle relaxation over the whole distribution with the characteristic time T_2 (Aniansson's slow process) brings the micelle distribution back to equilibrium.

The coverage σ is sketched as a function of time in Figure 6 showing the three successive adsorption regimes of the long-time kinetics.

VI. Conclusion

We have studied the adsorption kinetics of diblock copolymers onto a wall from a highly selective solvent when the insoluble A block adsorbs and the soluble B block is repelled by the wall. In the bulk the critical micellar concentration is extremely low and at any reasonable concentration the polymer chains aggregate to form micelles. The essential results of our study concern the role of micelles on the adsorption kinetics. Micelles never adsorb directly: the external layer soluble in the solvent is repelled strongly by the wall and creates an enormous energy barrier for adsorption that we studied in section III. In a reasonable experimental time scale, only the free chains adsorb. This however does not mean that the micelles play no role on the adsorption kinetics. The adsorption of free chains locally breaks the equilibrium between free chains and micelles. The local equilibrium is restored by a relaxation of the micelles, which release free chains that may themselves adsorb. The presence of micelles thus accelerates strongly the formation of the adsorbed copolymer layer on the wall. This effect is particularly important in the early stages of the adsorption when the interfacial layer has not yet developed the brush structure that presents a high-energy barrier to the adsorption of new chains.

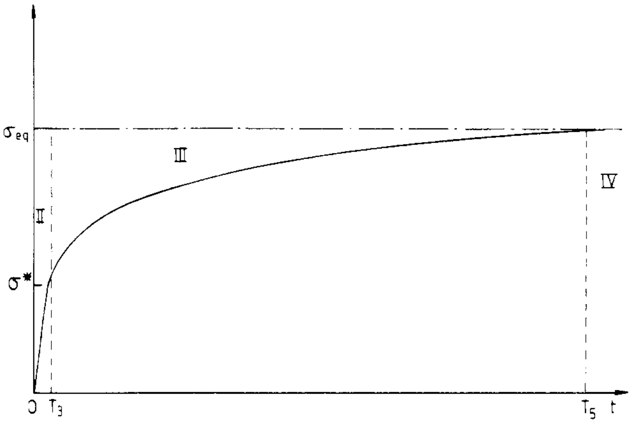

Figure 6. Sketch of the long-time adsorption kinetics showing the surface coverage in the micelle-limited regime II ($T_1 \simeq 0 < t < T_1$), the brush-limited regime III ($T_3 < t < T_5$), and the saturation regime IV ($t > T_5$).

In order to describe the relaxation of micelles, we have used a generalization of the work of Aniansson[14-17] on small surfactant micelles first used for copolymers by Halperin and Alexander.[18,19] This leads in the regime where the micelle relaxation is the limiting step for the adsorption to a linear increase with time of the surface coverage, σ, much faster than the adsorption of a free-chain solution, which is diffusion limited and would increase with time as $t^{1/2}$.

At later times, the rate-limiting step for the adsorption is the energy barrier presented by the polymer brush formed by the adsorbed chains. The increase of the surface coverage is very slow [as $(\log t)^{6/5}$], and micelles play little role in this regime. This extremely slow increase of the surface coverage should not allow the formation of the equilibrium brush structure in a reasonable time in many experiments. For block copolymer solutions the various time scales characterizing these adsorption regimes are well separated; this allows an asymptotic analysis. We do not expect it to be true for small-chain surfactants, and their behavior is probably qualitatively very different.

Our results could be directly compared with experiments on diblock copolymer adsorption. The only experiment that we know of where the amount of adsorbed copolymer is measured as a function of time is due to Tassin[13] et al. for polystyrene–poly(vinylpyridine) copolymers in toluene solution. The adsorption kinetics strongly depends on the concentration and becomes faster above the cmc, the differences being particularly important in the early stages of the adsorption (at times of the order of 100 s). At later times (up to 15 h where the experiment is stopped) the surface coverage increases logarithmically with time. One should, however, notice that we have supposed throughout the paper that the dense polymer regions formed by the core of the micelles or the adsorbed layer remain liquid; it is not clear whether this is true experimentally.

Our analysis has been quite rough, as we were limited to scaling laws, and several points certainly deserve a more precise study. This is particularly the case for the micelle relaxation phenomena, which seem to have received very little attention both on the theoretical and the experimental side. The potential barrier created by the adsorbed polymer brush could also be studied in more detail by using the more refined theory of Milner et al.[33,34] as has been done for end-grafted polymers by Ligoure and Leibler.[35] This would allow a determination of prefactors that can play an important role in the exponential Boltzmann factor if one wants to give qualitative numerical estimates. The adsorption kinetics has been described by a diffusion equation, ignoring any convective motion in the solvent. Convective motions certainly exist in practice far from the solid surface and accelerate the transport of chains toward the surface.

Finally we have limited the study to highly selective solvents where the copolymer block that is incompatible with the solvent forms molten regions and to adsorption from a micellar phase in order to get a more realistic approach; we should certainly extend this work to less selective solvents and to solutions forming other types of mesophases.[8]

Acknowledgment. We have benefited from useful discussions on micelle relaxation with J. Lang and R. Zana, on the interaction between a micelle and a wall with P. Pincus, and on the experimental aspects of copolymer solutions with E. Pfefferkorn, A. Schmitt, and R. Varoqui. It is a pleasure to thank them. We also want to thank L. Leibler and C. Ligoure for constructive comments and for sending us a copy of their work prior to publication.

Appendix I. Interaction between a Solid Wall and a Starlike Micelle in the Mean-Field (Random-Walk) Approximation

In the mean-field (random-walk) approximation, the propagator of a free chain with one end fixed at the origin is Gaussian. When two coordinates are integrated out, we obtain the probability of finding the other end at the abscissa z after N steps

$$G_N{}^0(z) = (3/2\pi a^2 N)^{1/2} \exp(-\mathbf{z}^2) \qquad \text{(AI-1)}$$

where N is the number of statistical units (persistence lengths) in the chain and $\mathbf{z}$ is the reduced distance to the plane $z = 0$:

$$\mathbf{z} = (3/2Na^2)^{1/2} z \qquad \text{(AI-2)}$$

If the plane $z = 0$ is replaced by an impenetrable wall, when one end of the chain is fixed at a distance d from the wall, the probability of finding a monomer at the wall is zero. The propagator is the solution of the diffusion equation such that $G_N(0) = 0$. Using an image picture, we obtain

$$G_N(z) = Z^{-1}(G_N{}^0(z-d) - G_N{}^0(z+d)) \qquad \text{(AI-3)}$$

Usual normalization gives the partition function Z of a chain with one end fixed at a distance d from the wall and the other free in the half-space:

$$Z(d) = \operatorname{erf} \mathbf{d} \qquad \text{(AI-4)}$$

The last relation defines the free energy, $F(d)$, of a chain with one end fixed at a distance d from the wall and the other free in the half-space

$$F(d) = -kT \log (\operatorname{erf} \mathbf{d}) \qquad \text{(AI-5)}$$

where the reference state is taken infinitely far from the wall.

When p such noninteracting chains are grafted on a pointlike core located at a distance d from the wall, to build a starlike micelle, their partition function Z_p is

$$Z_p = Z^p \qquad \text{(AI-6)}$$

and therefrom the free energy

$$F(d) = -pkT \log (\operatorname{erf} \mathbf{d}) \qquad \text{(AI-7)}$$

Expanding the error function for small $\mathbf{d}$, we find, for the partition function and the free energy

$$Z_p(d) = [(6/\pi)^{1/2} d/R]^p \qquad \text{(AI-8)}$$

$$F(d) = -pkT \log [(6/\pi)^{1/2} d/R] \qquad \text{(AI-9)}$$

where the micelle radius, R, is

$$R = (Na^2)^{1/2} \qquad \text{(AI-10)}$$

For distances d small compared to R the numerical factor in the logarithm function becomes negligible. As announced, this result follows the general scaling form of eq III-1, the mean-field exponent being $m_0 = p$. The introduction of the excluded-volume interaction only changes the value of the exponent and thus the prefactor of the logarithm function in the free energy, replacing p by $p^{3/2}$ (compare eqs III-5 and AI-9, for instance).

Appendix II. Explicit Calculation of the Chain Concentration Profile and the Surface Coverage in the Diffusive and the Micelle Regime

Here we present an explicit calculation of the concentration profile and the coverage in the low-coverage regimes where the potential barrier due to the brush is not relevant. In this aim we assume linear micelle relaxation (nonlinear relaxation is considered in Appendix III); furthermore, we replace the ratio of the characteristic times for micelle relaxation and diffusion through the barrier by a constant:

$$T_1/(K^2/D) = \alpha^2 \qquad \text{(AII-1)}$$

We consider here regimes where the potential barrier is not relevant, so in our calculation we let α go to infinity. Micelle relaxation defines a time scale T_1 and a length scale $(DT_1)^{1/2}$; using these units, we write the relaxation–diffusion equation (eq V-4) in a dimensionless form

$$\frac{\partial f}{\partial \tau} = \frac{\partial f}{\partial y^2} - f \qquad \text{(AII-2)}$$

where $\tau = t/T_1$ and $y = z/(DT_1)^{1/2}$. When the Laplace transform of $h(\tau)$ is denoted by $\mathbf{h}(s)$, the transform of eq AI-2 reads

$$s\mathbf{f}(s,y) = \frac{\partial^2 \mathbf{f}}{\partial y^2}(s,y) - \mathbf{f}(s,y) \qquad \text{(AII-3)}$$

The solution $\mathbf{f}(s,y)$ must vanish at infinity and is thus

$$\mathbf{f}(s,y) = B(s) \exp[-y(1+s)^{1/2}] \qquad \text{(AII-4)}$$

where $B(s)$ is determined by the boundary condition at the wall (eq V-6). Expressing this boundary condition by means of the Laplace transforms, we obtain

$$B(s) = \{s(1 + (1+s)^{1/2}/\alpha\}^{-1} \qquad \text{(AII-5)}$$

which in turn leads to the following expression of $\mathbf{f}(s,y)$

$$\mathbf{f}(s,y) = \frac{\alpha \exp(-yS^{1/2})}{(s-1)(S^{1/2} + \alpha)} \qquad \text{(AII-6)}$$

where $S = s + 1$.

Coming back to the function of time $f(\tau,y)$, we obtain[36]

$$f = \exp(-\tau)\left\{\alpha\frac{\exp(-y+\tau)}{2(\alpha+1)}\operatorname{erfc}\left(\frac{y}{2\tau^{1/2}} - \tau^{1/2}\right) + \alpha\frac{\exp(y+\tau)}{2(\alpha-1)}\operatorname{erfc}\left(\frac{y}{2\tau^{1/2}} + \tau^{1/2}\right) - \frac{\alpha^2}{\alpha^2-1}\exp(\alpha y + \alpha^2\tau)\operatorname{erfc}\left(\frac{y}{2\tau^{1/2}} + \alpha\tau^{1/2}\right)\right\} \quad \text{(AII-7)}$$

Let us first show that the concentration is time independent near the wall for times larger than T_1. More generally, at a point y for times τ larger than $y/2$, using the complement error function erfc[36] with positive argument, we obtain from the above formula

$$f = \frac{\alpha\exp(-y)}{\alpha+1} - \alpha\frac{\exp(-y)}{2(\alpha+1)}\operatorname{erfc}\left(\tau^{1/2} - \frac{y}{2\tau^{1/2}}\right) + \alpha\frac{\exp(y)}{2(\alpha-1)}\operatorname{erfc}\left(\frac{y}{2\tau^{1/2}} + \tau^{1/2}\right) - \frac{\alpha^2}{\alpha^2-1}\exp[\alpha y + (\alpha^2 - 1)\tau]\operatorname{erfc}\left(\frac{y}{2\tau^{1/2}} + \alpha\tau^{1/2}\right) \quad \text{(AII-8)}$$

Using the erfc function expansion for large arguments leads to

$$f = [\alpha/(\alpha+1)]\exp(-y)[1 + \epsilon(\tau,y)] \qquad \text{(AII-9)}$$

where

$$\epsilon(\tau,y) = \frac{\exp[-(\tau^{1/2} - y/2\tau^{1/2})^2]}{2\pi^{1/2}}\left\{\frac{\alpha+1}{\alpha-1}\frac{1}{\tau^{1/2} + y/2\tau^{1/2}} - \frac{1}{\tau^{1/2} - y/2\tau^{1/2}} - \frac{2\alpha}{\alpha-1}\frac{1}{\alpha\tau^{1/2} + y/2\tau^{1/2}}\right\} \quad \text{(AII-10)}$$

from which it clearly appears that $f(y,\tau)$ becomes τ independent for τ much larger than 1 and, as already assumed, τ larger than $y/2$ (the second term $\epsilon(\tau,y)$ being a very small correction). In particular, close to the wall the chain concentration is steady at times larger than T_1. When α is much larger than unity, we recover

$$f = \exp(-y) \qquad \text{(AII-11)}$$

a result obtained directly in the text.

From the expression of $f(y,\tau)$ we deduce the coverage rate

$$\frac{d\sigma}{dt} = -\frac{\Phi_{\text{cmc}}}{(DT_1)^{1/2}}D\frac{\partial f}{\partial y}(0,\tau) \qquad \text{(AII-12)}$$

or

$$\frac{d\sigma}{dt} = -\frac{\Phi_{\text{cmc}}}{(DT_1)^{1/2}}D\left[\frac{\alpha}{\alpha^2-1} - \frac{\alpha^2}{\alpha^2-1}\operatorname{erf}(\tau^{1/2}) + \alpha\exp[(\alpha^2-1)\tau]\operatorname{erfc}(\alpha\tau^{1/2})\right] \quad \text{(AII-13)}$$

in which the time-dependent term relaxes toward 1 as 1 + $[\exp(-\tau)]/(\pi\tau)^{1/2}$.

For times larger than T_1 we thus obtain

$$\frac{d\sigma}{dt} = \frac{\Phi_{\text{cmc}}}{(DT_1)^{1/2}}D\frac{\alpha}{\alpha+1} \qquad \text{(AII-14)}$$

an expression consistent with the previous result for large α. The short time limit (above the molecular regime) valid for $\alpha^{-2} \ll \tau \ll 1$ is dominated by the last term, where we obtain

$$\frac{d\sigma}{dt} = \frac{\Phi_{\text{cmc}}}{(\pi Dt)^{1/2}}D \qquad \text{(AII-15)}$$

which gives the coverage rate in the diffusive regime. It is however possible to deduce a simple expression for the coverage by using tabulated functions for $\tau \gg \alpha^{-2}$. Expanding the last erfc function for large arguments, we obtain the coverage rate:

$$\frac{d\sigma}{dt} = \frac{\Phi_{\text{cmc}}}{(DT_1)^{1/2}}D\left[\frac{\alpha}{\alpha+1} + \frac{\alpha^2}{\alpha^2-1}\left[\frac{\exp(-\tau)}{(\pi\tau)^{1/2}} - \operatorname{erfc}(\tau^{1/2})\right]\right] \quad \text{(AII-16)}$$

For convenience we go over to $\alpha \gg 1$; then

$$\frac{d\sigma}{dt} = \frac{\Phi_{\text{cmc}}}{(DT_1)^{1/2}}D\,g(\tau) \qquad \text{(AII-17)}$$

with $g(\tau) = 1 + [\exp(-\tau)]/(\pi\tau)^{1/2} - \operatorname{erfc}(\tau^{1/2})$.

The coverage may be deduced by integration

$$\sigma = \Phi_{\text{cmc}}(DT_1)^{1/2}G(\tau) \qquad \text{(AII-18)}$$

where $G(\tau) = \int_0^\tau g(u)\,du = \tau + \operatorname{erf}(\tau^{1/2}) - 2[1/4 - i^2\operatorname{erfc}(\tau^{1/2}) - \tau^{1/2}i^1\operatorname{erfc}(\tau^{1/2})]$, $i^n\operatorname{erfc}(x)$ being the tabulated, repeated integrals:

$$i^n\operatorname{erfc}(x) = \int_x^\infty i^{n-1}\operatorname{erfc}(u)\,du \qquad \text{with } i^0\operatorname{erfc}(x) = \operatorname{erfc}(x)$$

The plot of function $G(\tau)$ (see Figure 5) shows that it is close to its asymptotic form

$$G(\infty,\tau) = \tau + 1/2 \qquad \text{(AII-19)}$$

for $\tau > 1$; the linear regime is then reached. On the same figure we plot

$$G_{\text{ch}}(\tau) = 2/(\pi\tau)^{1/2} \qquad \text{(AII-20)}$$

corresponding to the extrapolated diffusive regime; one sees how much micelle relaxation accelerates the kinetics.

Appendix III. Effect of Nonlinear Micelle Relaxation on the Kinetics in the Micelle Regime

In this appendix nonlinear micelle relaxation and its effect on the adsorption kinetics are considered. In the text we use a linear law to describe Aniansson's fast relaxation process. This is written (eq II-21)

$$\partial\Phi_1/\partial t = (\Phi_{\text{cmc}} - \Phi_1)/T_1 \qquad \text{(AIII-1)}$$

where T_1 depends on both the extraction time τ for a single chain and the micelle distribution (see eq II-26). When the dimensionless concentration $f = (\Phi_{\text{cmc}} - \Phi_1)/\Phi_{\text{cmc}}$ is used, the above equation reads

$$\partial f/\partial t = -f/T_1 \qquad \text{(AIII-2)}$$

The right-hand side may be considered as a first-order expansion of a micelle relaxation term $s(f)$; when f remains close to zero the linear approximation is certainly valid, we now give a solution of the diffusion–relaxation equation (eq IV-1) beyond linearity:

$$\frac{\partial f}{\partial t} = D\frac{\partial^2 f}{\partial z^2} - s(f) \qquad \text{(AIII-3)}$$

Assuming a quasisteady profile near the wall, we neglect the left-hand side of AIII-3 and obtain

$$d^2f/dz^2 = s(f)/D \qquad \text{(AIII-4)}$$

which by integration leads to

$$\left[\frac{\partial f}{\partial z}(0)\right]^2 = 2\int_0^{f(0)} \frac{s(f)}{D}\,\mathrm{d}f \tag{AIII-5}$$

This in turn gives the flux to the wall

$$J(0) = D\Phi_{\mathrm{cmc}}\left(\frac{2}{D}\int_0^{f(0)} s(f)\,\mathrm{d}f\right)^{1/2} \tag{AIII-6}$$

We thus recover the linear micelle regime

$$\sigma = \frac{\Phi_{\mathrm{cmc}}D}{(DT)^{1/2}}t + c \tag{AIII-7}$$

with

$$T = \left[\int_0^{f(0)} 2s(f)\,\mathrm{d}f\right]^{-1} \tag{AIII-8}$$

Assuming a strongly depleted layer close to the wall, $f(0)$ can be set equal to 1 in the above integral:

$$T = \left[\int_0^{1} 2s(f)\,\mathrm{d}f\right]^{-1} \tag{AIII-9}$$

Note that T takes the particular value T_1 when $s(f)$ is replaced by its linear approximation f/T_1. In this picture all the results for the micelle regime hold if one replaces T_1 by T. However, the precise law for $s(f)$ has not been obtained so far to our knowledge.

We focus now on the special case $f = 1$, where the remaining free chains may be neglected, which requires a special treatment. The whole size distribution relaxes then, with the mean aggregation number moving toward 1. When polydispersity in the distribution peak is neglected, the associated relaxation term reads

$$\partial\Phi_1/\partial t = \Phi/n\tau(n) \tag{AIII-10}$$

where n is the instantaneous mean aggregation number and $\tau(n)$ the associated extraction time.

For $n = p$ we obtain, from eq II-26

$$\left.\frac{\partial\Phi_1}{\partial t}\right|_{n=p} = \frac{\Phi_{\mathrm{cmc}}}{T_1} \tag{AIII-11}$$

We checked (eq V-23) that for copolymer concentrations well above the cmc, as is usually the case, each micelle releases less than the average fluctuation δp of the size distribution chains. We may neglect the variation of $\tau(n)$ during the whole process, so we set $\tau(n) = \tau(p)$. Thus, for poor chain concentrations ($f \simeq 1$) the micelle relaxation term $s(f)$ tends toward its linear extrapolation $1/T_1$. This is due to the small amount of chains released by each micelle; we may assume that $s(f)$ remains close to the linear law everywhere or at least that the time T defined by the integral in eq AIII-9 remains of order T_1. The results for the micelle regime obtained under the linear relaxation assumption in section V2 must thus be valid.

Appendix IV. Comparison between Crossover Coverage and Equilibrium Coverage

To obtain the equilibrium coverage, we may equate the stretching energy of the B block in the brush $F(\sigma_{\mathrm{eq}})$ and the chemical potential of a chain in the solution μ_{cmc} using the notations introduced in eq II-27:

$$F(\sigma_{\mathrm{eq}}) = \beta N_{\mathrm{A}}^{2/5} \tag{AIV-1}$$

The crossover coverage, σ^*, is given by eq V-17; equating the arguments of the leading exponential factors coming from the activation energy, $F(\sigma^*)$, and the relaxation time T_1, we obtain

$$F(\sigma^*) = (\alpha/2)N_{\mathrm{A}}^{2/5} \tag{AIV-2}$$

As mentioned after eq II-27, α is smaller than β; thus σ^* is smaller than σ_{eq}, F being a monotonic increasing function of σ.

References and Notes

(1) Napper, D. H. *Polymer Stabilization of Colloidal Dispersions*; Academic Press: London, 1983.

(2) Pincus, P. Proceedings of the XVII Reunion de Fisica Estadistica, Oaxtepac, Mexico, 1988.

(3) Taunton, H. J.; Topakcioglu, C.; Fetters, L. J.; Klein, J. *Macromolecules* **1988**, *21*, 3333.

(4) Joanny, J. F.; Leibler, L. Proceedings of the 195th National Meeting of the Amercian Chemical Society, Toronto, June 5–10, 1988.

(5) Zana, R. *Surfactants in Solution*; Mittal, K. L., Bothorel, P., Eds.; Plenum Press: New York, 1986; Vol. 4.

(6) Lang, J.; Zana, R. *Surfactant Solutions. New Methods of Investigation*; Zana, R., Ed.; Dekker: New York, 1987.

(7) Tandford, C. *The Hydrophobic Effect*; Wiley: New York, 1980.

(8) Marquès C. M.; Joanny, J. F.; Leibler, L. *Macromolecules* **1988**, *21*, 1051.

(9) Mukerjee, P. *Phys. Chem.* **1978**, *82*, 931.

(10) Taunton, H. J.; Topakcioglu, C.; Fetters, L. J.; Klein, J. *Nature* **1988**, *332*, 713.

(11) Tirrell, M.; Patel, S.; Hadziioannou, G. *Proc. Natl. Acad. Sci.* **1987**, *84*, 4725.

(12) Hadziioannou, G.; Granick, G.; Patel, S.; Tirrell, M. *J. Am. Chem. Soc.* **1986**, *108*, 2869.

(13) Tassin, J. F.; Siemens, R. L.; Tang, W. T.; Hadziioannou, G.; Swalen, J. D.; Smith, B. A. *J. Phys. Chem.* **1989**, *93*, 2106.

(14) Aniansson, E. A. G.; Wall, S. N.; Almgren, M.; Hoffman, H.; Kielmann, I.; Ulbricht, W.; Zana, R.; Lang, J.; Tondre, C. *J. Phys. Chem.* **1976**, *80*, 905.

(15) Aniansson, E. A. G.; Wall, S. N. *J. Phys. Chem.* **1974**, *78*, 1024.

(16) Aniansson, E. A. G.; Wall, S. N. *J. Phys. Chem.* **1975**, *79*, 857.

(17) Aniansson, E. A. G. *Prog. Colloid. Polym. Sci.* **1985**, *70*, 2.

(18) Halperin, A. *Europhys. Lett.* **1989**, *8*, 351.

(19) Halperin, A.; Alexander, S. *Macromolecules* **1989**, *22*, 2400.

(20) Leibler, L.; Orland, H.; Wheeler, J. *J. Chem. Phys.* **1983**, *79*, 3550.

(21) Goldstein, R. E. *J. Chem. Phys.* **1986**, *84*, 3367.

(22) Bug, A. L. R.; Cates, M. E.; Safran, S. A.; Witten, T. A. *J. Chem. Phys.* **1987**, *87*, 1824.

(23) Daoud, M.; Cotton, J. P. *J. Phys. (Paris)* **1982**, *43*, 531.

(24) Lessner, E.; Teubner, M.; Kahlweit, M. *J. Phys. Chem.* **1981**, *85*, 1529.

(25) Witten, T. A.; Pincus, P. *Macromolecules* **1986**, *19*, 2509.

(26) Frisch, H. L.; Mysels, K. *J. Phys. Chem.* **1983**, *87*, 3998.

(27) Mysels, K.; Frisch, H. L. *J. Colloid Interface Sci.* **1984**, *99*, 138.

(28) Schaaf, P.; Déjardin, Ph. *Colloids Surf.* **1987**, *24*, 239.

(29) de Gennes, P.-G. *Scaling Concepts in Polymer Physics*; Cornell University Press: Ithaca, NY, 1979.

(30) Alexander, S. *J. Phys. (Paris)* **1977**, *38*, 977.

(31) Kramers, H. A. *Physica* **1940**, *7*, 284.

(32) Munsch, N. R.; Gast, A. P. *Macromolecules* **1988**, *21*, 1366.

(33) Milner, S.; Witten, T. A.; Cates, M. *Europhys. Lett.* **1988**, *5*, 413.

(34) Milner, S.; Witten, T. A.; Cates, M. *Macromolecules* **1988**, *21*, 2610.

(35) Ligoure, C.; Leibler, L., submitted for publication in *J. Phys. (Paris)*.

(36) *Handbook of Mathematical Functions*; Abramovitz, M., Stegun, A., Eds.; Dover Publications: New York, 1965.

(37) Halperin, A. *Macromolecules* **1987**, *20*, 2943.

(38) Halperin, A.; Alexander, S. *Europhys. Lett.* **1988**, *6*, 439.